J. Condensed Matter Nucl. Sci. 6 (2012) 241–255

Research Article

First-principles Studies of Electronic and Ionic Transport in Palladium Hydrides/Deuterides

N. Luo and George H. Miley*

Department of Nuclear, Plasma and Radiological Engineering, University of Illinois, Urbana, IL 61801, USA

Abstract

We review first principles studies on some transport properties and ion dynamics of the palladium hydride/deuteride system. The review is not meant to extensive, because it is aimed at understanding the abnormal and not-so-well-known part of the transport in the aforementioned compound that may be of particular importance to scientists studying Low-energy Nuclear Reactions (LENRs) as well as persons interested in hydrogen storage in metal hydrides. Many well-known properties of Pd/H, such as the steady-state electronic structure, have already been covered by numerous studies and reviews elsewhere. Many of the studies reviewed here were carried out at the University of Illinois. We focus on the three different but related topics: (1) The charge state of H in Pd, especially in the hopping process. (2) The electron–phonon interaction, and its role in the negative differential resistivity. (3) Defects and dislocations in Pd and their effects in the H state and its transport. The latter is of intellectual interest relative to our recent research on LENRs involving the conjectured formation of hydrogen/deuterium clusters in such defects.

Keywords: Electro-negativity, Electron–phonon interaction, Low-energy nuclear reaction, Palladium–hydride system

1. Introduction

The palladium–hydride system has been an interesting yet perplexing topic of multi-disciplinary research for many years [1–3]. This is a material system with many practical applications such as fuel cells, batteries, catalytic chemistry and nuclear chemistry. Also many controversies surround the particular palladium–deuteride system as for the possibility of low energy nuclear reactions. Unlike ordinary metal alloys, where a fairly good understanding is achieved through straightforward concepts, metal hydrides pose a number of complications. First, hydrogen is smaller and lighter than the host metals, and hence its motion in the host metals generates some unexpected effects, quantum ones included. Second, a hydrogen atom is a stronger attractor of electrons than most metal atoms. Therefore, the bonding nature between hydrogen and metals is different from that of a normal metal bond. Many other issues exist in the palladium–hydride system, which is finding increasing importance in various applications. For example, the unique hydrogen storage property of Pd plays an important role in fuel cells and storage battery development. The Pd alloys are often

*E-mail: nluo@illinois;ghmiley@illinois.edu

utilized as a hydrogen permeation selector, which is important to both carbon sequestration of the green energy field and hydrogen/deuterium/tritium (H/D/T) separation of the nuclear industry. The latter will play an important role with future D–T nuclear fusion reactors' coming into the age. In the well-established domain, the phenomena of hydrogen adsorption and the resulting catalytic properties of hydrogenated Pd surfaces, on one hand, pose a fundamental issue for the theoretical understanding of basic surface physics and catalytic chemistry, while on the other hand, are significant for technical applications such as the hydrocarbon industry. More recently, various properties of highly loaded Pd have been of intense interest in low-energy nuclear reaction (LENR) research. In that case issues range from transport of deuterium in the Pd (or other materials such as PdO, Ti, U, and Ni), their localization to form "reactive sites" methods for triggering or catalyzing reactions in these sites, and subsequent reaction kinetics [4,5].

Yet despite extensive research carried out on Pd/H over the past 50 years, some of its fundamental properties are still not well understood. Such problems include the charge state of hydrogen and charge transport of both electron and H ion in the Pd lattice, which are addressed here.

Before we get into the details of Pd/H transport, first we need a few words on the major computational tools that were employed. The general feature of these methods is that they are from first-principles, i.e., their foundation is the simple mathematical formulation of quantum mechanics. This means that empirical data, like electron hopping matrix elements, force field of the atoms, for example that of Pd, extrapolated from experiment and so on, are *not* utilized in the calculation of electronic structures and simulation of atomic motion. Instead, all of the data are calculated from the simple fact that there are 46 electrons outside the Pd nucleus. Therefore, they are full quantum mechanical treatment of the condensed matter system. However, the many-body problem cannot be fully analytically solved. There must exist some simple approximations yet accurate enough so that a real-world calculation can be carried out. A broad range of approximations based on the Hohenberg–Kohn theorem [6] forms the density functional theory (DFT) approach to solving many-body problems. In this regard, most software tools employed in the study are first-principles (sometimes all termed ab initio) DFT packages for electronic structure and molecular dynamics. In solving the many-body problem, the total Hamiltonian can be projected to different Hilbert spaces to facilitate the computation, taking advantage of various symmetries that exist in the specific problem. Then we have DFT based on different basis sets: plane-wave pseudopotential, augmented plane wave, linear combination of atomic orbit, Gaussian orbitals and so on. Such terminology will be often encountered later in the review.

2. Charge Transport and the Charge State of Hydrogen in Pd

Charge transport in palladium hydride (and metallic hydrides in general) is complicated in that it involves both electrons and H ions. Electron transport in PdH is complex and not anticipated as is manifested by the unusual electric resistance change versus the H/Pd ratio, illustrated conceptually in Fig. 1. As shown, the normalized resistance as a function of loading x, i.e. H/Pd atomic ratio, first increases and then decreases [7]. Further, it was recently observed that the resistance, finally undergoes an oscillation at ultra high loadings [8]. As the mobility and the number of electrons in PdH are orders of magnitude higher than those of the H ion, electron transport dominates these resistance changes. The initial increase in the resistance (up until $x \sim 0.65$) is relatively easy to understand from an alloying point of view. Or, in other words, the added H in the lattice creates scattering centers, increasing the resistance. The subsequent drop for $x > 0.65$ is not completely understood, but is typically thought to be associated with the formation of new band states. The recently reported oscillation region shown in Fig. 1 has not yet been explained theoretically.

The instability is of particular interest since it could result in coherent oscillations that can accelerate the partially ionized hydrogen in the lattice like in a beat wave accelerator. The resulting high proton energy could well push the deuteron/palladium system far from the equilibrium, which in turn generates many unexpected phenomena.

In addition to resistivity studies, considerable research has been dedicated to probing the nature of H transport (e.g. diffusion and drift) in Pd. Original drift experiments [9,10] strongly suggest that H drifts in Pd in the form of a positive

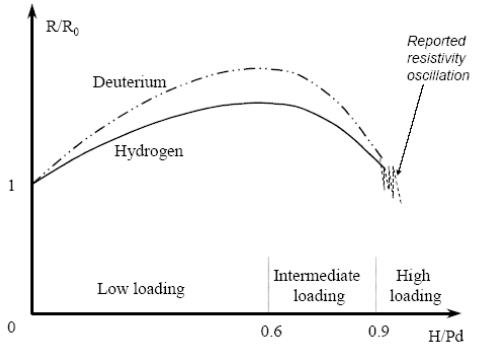

Figure 1. Normalized resistance R/R_0 vs. loading x, where R_0 is the initial resistance without loading. The solid curve is for hydrogen loading with the dot-dashed one for deuterium.

ion with a fractional charge number around +0.5, while a more recent study [11] gives +0.7. These observations, combined with the decrease of the paramagnetic susceptibility with H loading, strongly support the notion of a proton model in which the hydrogen is viewed as donating its electron to the unfilled Pd d-shell. However, such a proton model seems oversimplified in terms of experiments like the electronic specific heat [12]. As the electronic specific heat is directly proportional to the size of the Fermi surface, the proton model should predict a progressively smaller electronic specific heat as the H loading is increased. However, the contrary effect is found in the closely related nickel–hydride systems. Moreover, from a chemistry point of view, H can in principle acquire an electron from the host Pd because of its relatively large electro-negativity. Table 1 summarizes the relevant electronic properties of atomic Pd and H.

Some previous band structure calculations [12–18] have been carried out to elucidate the charge state of H in Pd. The studies include PdH and $PdH_{0.25}$, where unit cells can be easily defined. The general conclusion is that in these cases the H is slightly negatively charged in spite of the filling up of the Pd d-bands. Without further study, this result has appeared to contradict some of the observations made in H drifting experiments.

In [19], the authors provide improvements over previous band-structure calculations with more hydride compositions and proton locations considered. The authors also suggested how to reconcile the conflicting picture of a negative H ion inferred from electronic-structure calculations with the positive charge suggested by the hydrogen drift experiment.

3. Charge State of Hydrogen in Pd

Details of the calculation can be found in Ref. The explicit consideration of the so-called "bridging" site, designated in Fig. 2, was considered. This site, along with the two others, namely the "on-top" site and the "hollow" site, play an important role in the surface catalytic chemistry of Pd (1 0 0) surface.

The bridging site is considered here for one additional reason. The drift of hydrogen through interstitial hopping

Table 1. The work function of Pd metal and some related constants for atomic Pd and H.

	Electron affinity (eV)	Ionization energy (eV)	Electronegativity (Pauli scale)	Electronegativity (Allred–Rochow scale)
Pd Atom	0.518	7.76	2.2	1.35
H Atom	0.702	13.6	2.2	2.2
Work function of Pd metal (eV)			5.12	

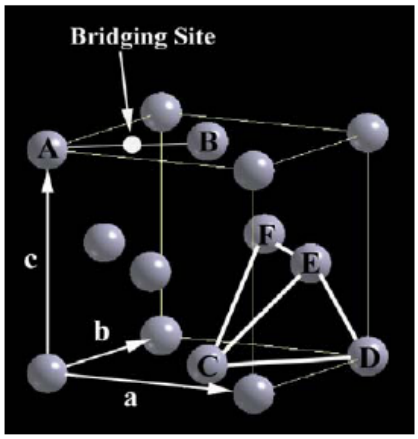

Figure 2. The so-called bridging site in the Pd face centered cubic lattice.

inside a Pd metal matrix is a dynamic process, and hydrogen atoms likely pass through one of two possible sites: the bulk tetrahedral site or the bridging site. Since the path through the bridging site is the shortest, it is of special interest to probe the electronic structure of H located at this site. Prior studies have generally assumed, without proof, that hopping mainly occurs through the tetrahedral site, even though the bridging site path is shorter. The charge state of H at the tetrahedral site was calculated for the first time too, because H is likely to hop through this site as well. Indeed, we will see later that compared with the bridging site, it is an energetically more favorable path. Also, PdH_x of three different compositions x, namely, $PdH_{0.25}$, $PdH_{0.5}$, PdH are studied when the H is at the octahedral site. This was done to investigate the change of charge density around H as the loading proceeds. A careful choice of super-cell was necessary for $PdH_{0.5}$ so as to maintain the inversion center. H atoms are added in the Pd lattice in such a way that the super-cell is kept as small as possible. The existence of the inversion center helps keep the calculation in real numbers and the convergence of the computation is much easier at a result.

We expect less charge around the H when the hydrogen fraction, x, decreases, because the electron around the H has to be shared by more Pd. From Table 2, this is indeed what happens. However, the magnitude of change is less than what is expected from a simple consideration of the work function, electron affinity and electro-negativity. As the electron affinity of a single H, 0.702 eV, is much smaller than the work function of a Pd metal, 5.12 eV, an electron tends to shift away from H when the H composition x is small. However, the DFT result for $PdH_{0.25}$ does not show much of this tendency. Our explanation is that in the calculation the H is always eight-coordinated in all three loadings, and intercepts roughly the same portion of Pd orbits. Therefore, the change in the charge state is quite small although the actual loading has been significantly altered.

The radius of the muffin-tin sphere is taken as 1.5 Bohr. For reference, previous calculations deal only with partial

Table 2. Charge and corresponding δ (defined by $H^{\delta-}$) in the H muffin-tin spheres in different compositions and locations.

Case	$PdH_{0.25}$	$PdH_{0.5}$	PdH	PdH (bridging)	PdH (etrahedral)
Charge (e unit)	1.13	1.18	1.22	1.81	1.56
δ	0.13	0.18	0.22	0.81	0.56

charge from the lowest band and are, therefore, lower than the values shown here. Ref. [14] gives a partial charge of 0.67 for a radius of 1.35 Bohr while [15] has a partial charge of 0.68 at 1.6 Bohr.

The charge density distribution in one of the (1 0 0) planes is given in Fig. 3(a)–(c) for each of the three cases. The hydrogen is slightly negatively charged in all of these cases and the change with loading is hardly noticeable. To represent these cases, the charge state can be labeled as $H^{\delta-}$, where δ- is often a small fraction. In the case of octahedral H, for example, δ ranges from 0.1 to 0.2. (see Table 2). This result qualitatively corroborates both the APW conclusion of [14] and the pseudopotential result of [15]. The results confirmed the formation of negatively charged H in Pd. A direct and quantitative comparison with their results is, however, not possible so far because both authors quoted the charge for the lowest band only, which underestimates the total charge around H.

In Fig. 3, the labeling of the horizontal axes is in percentage of the FCC cell lengths in (1 0 0) planes. The distance between the Pd atoms is about 2.8 Å. The scale for the vertical axis is electron charge per atomic unit volume. In Fig.

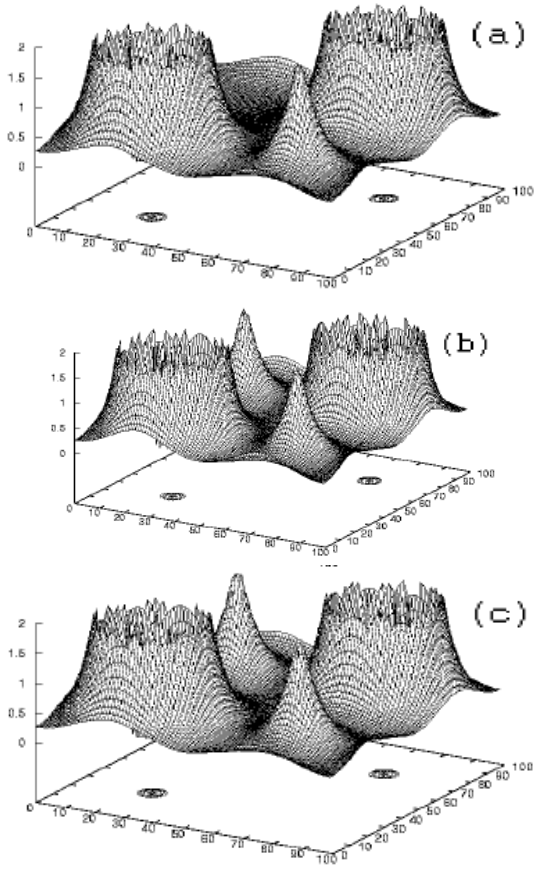

Figure 3. The charge distribution around octahedral H site, in one (1 0 0) plane of (a) $PdH_{0.25}$; (b) $PdH_{0.5}$; and (c) PdH.

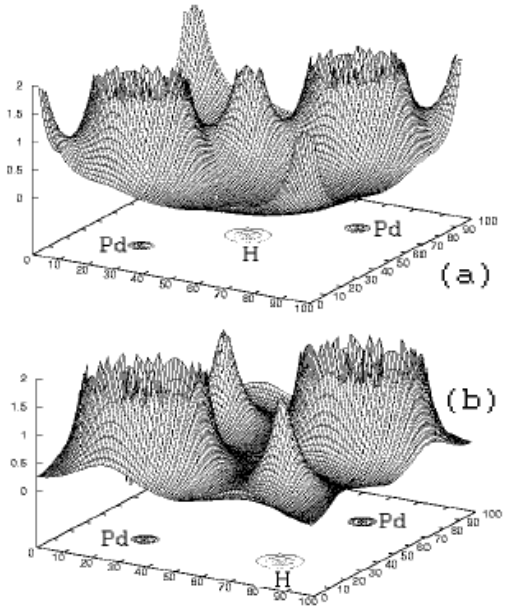

Figure 4. The charge distribution around: (a) bridging-site hydrogen and (b) tetrahedral-site hydrogen in one (1 0 0) plane of hypothetical PdH.

.

3(a), the H/Pd ratio in this particular (1 0 0) layer is 1:2, but that in the nearest-next neighbor layers is 0 and thus the bulk H/Pd ratio is 1:4. In Fig. 3(b), the H/Pd ratio in this particular (1 0 0) layer is 1:1, but that in the nearest-next neighbor layers is 0 and thus the bulk H/Pd ratio is 1:2.

This negatively charged H from a static band-structure calculation must be reconciled with the notion of a fractionally charged positive H ion found in drift experiments. This requires consideration of the dynamic nature of the proton hopping process. When an electric field is applied to the $H^{\delta-}$ at the octahedral site, the proton hopping (tunneling) process will be assisted in the direction of the field. Therefore, the hydrogen drift (or, in other words, an electric field assisted tunneling process) is characterized as that of a proton, i.e. a^{+1} charge, at the octahedral site. However, in hopping from one octahedral site to another, the proton likely follow a path through either the tetrahedral site or the bridging site, and the charge state at these two locations will also affect the path average charge of the hydrogen in a drift experiment. If the path is through the bridge site, there will be more negative (electron) charge around it as plotted in Fig. 4(a). Table 2 shows that the proton is roughly charged with 0.6 more electrons at the bridging site than at the octahedral site. This implies that the proton carries an effective electron cloud of -0.6 with it as it goes through the bridging region. Hence, the net proton charge manifested in this drift path is 1–0.6 $\sim$ 0.4. However, other possible paths all contribute. Therefore, the experimentally observed net charge Z^* should be a weighted average of paths through all possible sites.

The scales of axes in Fig. 4 are the same as those in Fig. 3. The horizontal locations of Pd and H atoms are, respectively, indicated with the corresponding labels. In Fig. 4(b), the H layer is roughly a quarter FCC Pd lattice constant from the (1 0 0) layers, and therefore, no Pd atom is shown in the plot.

The calculation of the effective charge in the drift experiments can be effected in a mathematical way. In the

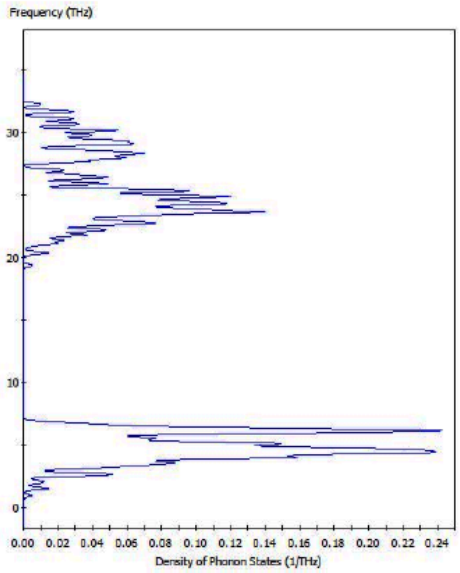

Figure 5. (a) The phonon density of states in PdH.

following explicit derivation, the weighted average is a sum as:

$$Z^* = \sum_i w_i[1 - (\delta_{\rm i} - \delta_{\rm o})]. \tag{1}$$

Here, Z^* is the effective charge found in drift experiments, and i the site indices. δ_i is the fractional charge of H on sites, where the hopping must pass through, as given in Table 2, and δ_o the fractional charge at the octahedral sites. w_i, the statistical probability of taking a path through site i, is given by the following,

$$w_i = \frac{{\rm e}^{-(E_{\rm i} - E_{\rm o})/KT}}{\sum_i {\rm e}^{-(E_{\rm i} - E_{\rm o})/KT}}, \tag{2}$$

where K is the Boltzmann constant and T the temperature. $E_{\rm o}$ is the energy of H when it is at the octahedral site and E_i the energy at site i.

To find out the energy of H at different sites, the linearized augmented plane wave package WIEN2K [20] was used to carry out a total energy study for H at each of the three sites. The resulting energy shift, the difference in total energy between H at a specific site and the reference octahedral site, is given in Table 3.

$E_{\rm t}$, $E_{\rm b}$, and $E_{\rm o}$ are energies, respectively, for tetrahedral, bridging and octahedral sites. Ref. [21] gives $E_{\rm t} - E_{\rm o} \sim 0.1$ eV, to which our result closely matches. $E_{\rm b}$–$E_{\rm o}$ has not been studied before to the best of the authors' knowledge.

As hoppings are mainly through the bridging and the tetrahedral sites, the right-hand site of Eq. (1) has essentially two terms

$$Z^* = w_{\rm t}[1 - (\delta_{\rm t} - \delta_{\rm o})] + w_{\rm b}[1 - (\delta_{\rm b} - \delta_{\rm o})], \tag{3}$$

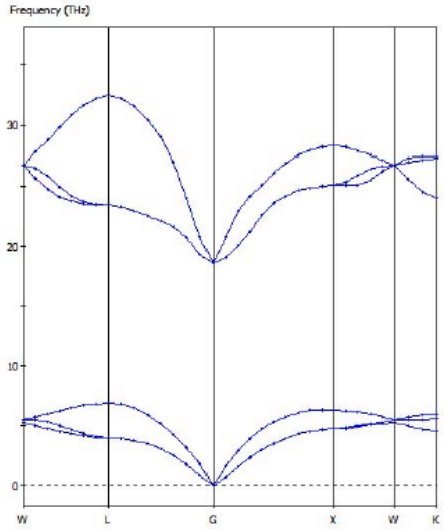

Figure 6. (a) The phonon dispersion (or band structure) along a few high-symmetry directions in the BZ.

where t and b are, respectively, indices for the tetrahedral and bridging sites. The tetrahedral δ_t is given by the last column of Table 2, and the general charge plot around the tetrahedral H is typified in Fig. 4(b). Because $E_b - E_o/KT$ is much larger than $E_t - E_o/KT$ at room temperature, the contribution from hopping via the bridging site is actually fairly small. Therefore, Eq. (3) simplifies to

$$Z^* = [1 - (\delta_t - \delta_o)] \tag{4}$$

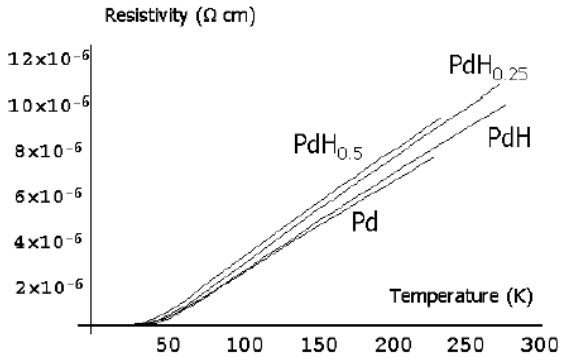

Figure 7. The temperature dependence of resistivity at different loadings.

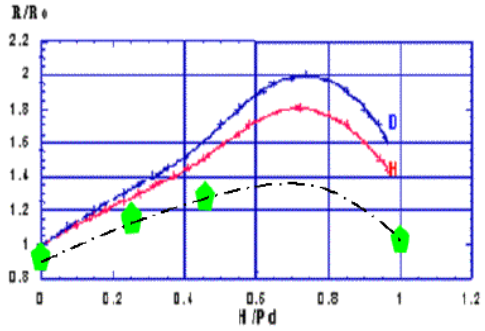

Figure 8. The normalized resistivity at different H loadings.

for ordinary experimental conditions. A simple calculation gives $Z^* \sim 0.7$, which is not far from the traditional average of 0.5 and closely matches the latest experiment results [10].

The negative charge of hydrogen found in the band-structure calculation is a *static* property in a condensed state, which is actually shared with all the coordinated Pd. One the other hand, the positive charge manifested in the proton drifting experiment is a dynamic property, because the proton obvious cannot carry all the negatively charged electrons and move around freely. Overall, the author's study served as a first step towards resolving certain problems involved in transport properties for the palladium–hydride system.

4. Resistivity from Electron–phonon Interaction

A significant part of the resistance of PdH is from the electron–phonon interaction. The first step in understanding the role of phonon in PdH is the phonon spectrum of the density of states. Because hydrogen or deuterium is the lightest

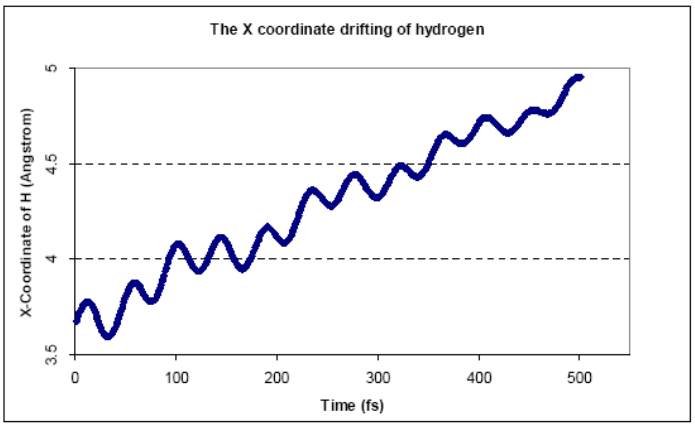

Figure 9. An exemplary coordinate change of H in Pd versus time. It is simulated in a micro-canonical ensemble, assuming an initial energy of 293 K for the H.

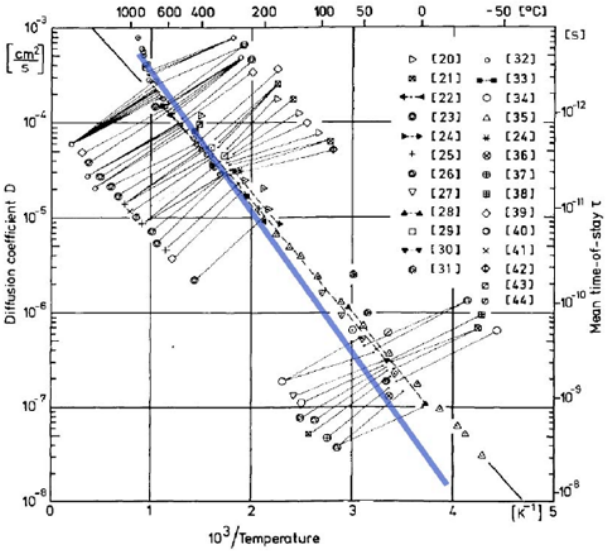

Figure 10. Calculated hydrogen diffusion constants with first-principles molecular dynamics. The *blue line* is obtained by connecting and extrapolating the calculated results at 0˚C and 800˚C. The width of the line roughly represents the statistical spread at different calculations.

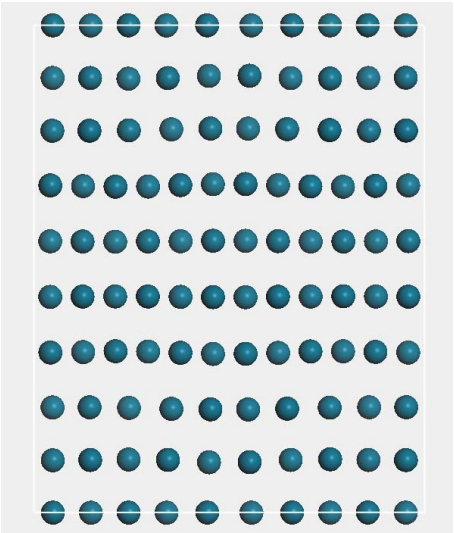

Figure 11. A dislocation along [2 1 1] in the FCC lattice of Pd, structural-optimized with CASTEP.

among all elements one expects phonons of quite high energy play an important role. Also helpful is the phonon dispersion relation along the high symmetry directions in the Brillouin zone (BZ). Both properties can be calculated by the plane-wave pseudopotential method, with the results plotted in Fig. 5.

The results of Fig. 5 are calculated with CASTEP in the linear response regime by assuming PdH being essentially an insulator. Although this is quite far-fetched assumption, the general phonon band is qualitatively similar to more accurate methods, such as the finite displacement approach, which is nevertheless more time consuming.

With the previous studies investigating the phonon dispersion and density of state of Pd and PdH, we can proceed with one more step ahead with the electron–phonon coupling constant, at different loading x. Our objective is to explain the experimental ρ–x curve, through a first-principles study of the electron–phonon coupling strength.

4.1. Theoretical basis of electric resistivity

Without considering any interband e-e scattering, the resistivity of a metal is given by the Bloch–Gruneisen formula,

$$\rho(T) = \rho_0 + \lambda_{\mathrm{tr}} \frac{4\pi}{\omega_{\mathrm{p,D}}^2} \frac{128\pi (k_{\mathrm{B}} T)^5}{(k_{\mathrm{B}} \Theta_{\mathrm{D}})^4} \int_0^{\theta_{\mathrm{D}}/2T} \frac{x^5}{\sinh^2 x} \mathrm{d}x, \tag{5}$$

where λ_{tr} is the dimensionless electron–phonon coupling constant. ρ_0 is the residual resistivity at absolute temperature 0 K, attributed to scattering from lattice impurities. $\Theta_{\mathrm{D}} \propto \sqrt{\text{bulk modulus/mass density}}$ is the Debye temperature, readily calculated if bulk modulus k is known.

$$\omega_{\mathrm{p,D}}^2 = \frac{4\pi n e^2}{m}$$

the plasma frequency is actually the measurement of the number of band carriers n, including both electron and hole in the case of Pd. Note that in Eq. (5), n and m, the band mass of relevant carriers, can be calculated from the band structures at and near the Fermi surface, which is routinely available from a typical electronic-structure package. The bulk modulus k is, strictly speaking, a function of temperature, but here it can be simply approximated by $\partial U \big/ \partial V$, where U is the total energy and V the crystal volume. Therefore, a straightforward volume-dependent total energy study using WIEN2K and other tools like CASTEP determine the value of k.

The electron–phonon coupling is one of most intensive parts of the computation. An often utilized method is the frozen-phonon approach. In this method, one has to find out the phonon normal modes of the relevant crystal. By distorting the lattice to the deformed types dictated by the normal modes, one can calculate the relevant energy change in the electronic band. The proportion between the band change and lattice change is directly related to the electron–phonon coupling. However, this approach is very time-consuming, sometimes prohibitive. The second and often-adopted means is the perturbative DFT, which is often faster at minimal sacrifice of accuracy. This is the method we adopted for this study.

Table 3. Energy shifts between different sites from total energy study.

Shifts	Energy (eV)
E_{t}–E_{o}	0.08
E_{t}–E_{o}	0.86

Table 4. Plasma frequency, Debye temperature and electron–phonon coupling constant at different H loadings.

	Pd	$PdH_{0.25}$	$PdH_{0.5}$	PdH
$\hbar\omega_{p,D}$(eV)	7.68	7.34	7.03	7.80
Θ_D(K)	281	293	304	328
λ_{tr}	0.47	0.51	0.52	0.54

4.1.1. *Calculation of electron–phonon coupling*

For n and m, the eigenvalues of bands that cross the Fermi surface were calculated at 140 k points in the irreducible Brillouin zone (IBZ). The band mass tensor is then calculated by an interpolation scheme near the Fermi surface. The IBZ k points are then generalized to the whole BZ in order to find out the effective carrier number of the relevant bands. The resulting n and $m$are listed in the first two rows of Table 1.

The electron–phonon coupling is treated perturbatively using the Planewave Self-consistent Field (PWSCF) package. The norm-conserved pseudopotential (PP) of Pd used in the calculation is obtained from Paolo Giannozzi's PP code. To ensure the transferability, the PP was tuned by calculating the band structure of Pd using PWSCF until a satisfactory comparison with the WIEN2K band is achieved. The result is given in the last row of Table 1.

The trend seen in electron–phonon coupling versus loading can be understood from other experimental facts. Pure Pd is not superconductive but a stoichiometric PdH has a critical temperature T_c of 9 K. This change indicates stronger electron–phonon interaction at higher H loading. Therefore, the theoretical λ_{tr} result given in Table 1 is confirmed by the trend in the superconducting transition temperature.

The plasma frequency Θ_D, or in other words, the total number of charge carriers keeps decreasing up to $x \sim 0.5$, then a rise is seen with x reaching 1. This can be understood from the band filling process with H is added in Pd. Palladium has three predominantly d-bands traversing the Fermi level. The fourth and fifth band have hole-like Fermi surface while that of the sixth is electron-like. At low loading, the added electrons from hydrogen mainly fills up the two hole bands, resulting in a decrease in the number of hole, which outpaces the increase in the electron number of the sixth band. Therefore, a reduction in the total number of current carrier happens, causing a decreasing plasma frequency with increasing loading. At $x = 0.6$, however, the two lower bands are now largely full, the increase in the electron number of the sixth band now more than offsets the loss in the hole number, and therefore $\Theta_D$begins to increase.

Substituting the calculated parameters into Eq. (1), the temperature- dependent resistivity is then derived for various loadings as shown in Fig. 4. The linear temperature dependence is the characteristic of a phonon-induced resistivity when temperature is on the order of a few hundred degrees Kelvin.

Alternatively, the normalized loading-dependent resistance at the room temperature is given in Fig. 5. The absolute values of theoretical results are well below the experimental ones. It is not a surprise considering the additional scattering from the H-induced disorder and the inter-band electron–electron scattering not included in the calculation.

The resistivity (resistance) of Fig. 7 is normalized to that of pure Pd at 300 K. The red and blue curves are from experiments. Theoretical results are given as the four pentagons. The black dot-dashed line is the theoretical least-square fit.

5. Ionic Dynamics

The ionic or molecular dynamics of hydrogen and its isotopes in metal lattices is a very interesting topic and of practical importance. It has broad applications such as metal hydride hydrogen storage, carbon dioxide sequestration, catalytic chemistry and should play critical role in future nuclear fusion power plants. A clear understanding of various aspect of such a process is therefore highly desired.

The experimental data of hydrogen diffusion in metals, especially palladium, have long been in existence in the

literature. However, a theoretical and computational understanding of such experimental results is far from adequate. Here, we describe some of the authors' on-going studies as an effort to unravel the relevant physics in first principles.

The hopping or diffusion of H in solid-state lattices is a dynamic process, and belongs to the very broad domain of molecular dynamics. Note that H for the most of time transport in the metal lattice in a partial charged (ionic) form. Therefore, the more precise term might instead be "ionic dynamics", when we are dealing with hydrogen in metals.

This problem can be addressed from first principles. In essence, a plain-wave pseudopotential method, CASTEP, based on the density functional theory can be utilized to find the electronic structure (energy eigenstates, charge density, etc.) of hydrogen in metals. The Car-Parrinello molecular dynamics method is resorted to in calculating the ionic force field. Afterwards, the statistic averages of a few correlation functions are calculated by the MDTEP package to yield important parameters such as diffusion coefficients. A typical MD simulation gives time-dependent variation of the H location as depicted in Fig. 8. The results can then be utilized to calculate the mean square displacement (MSD) of the hydrogen.

The MSD is related to the diffusion constant by a very simple relation

$$D = \frac{\mathrm{d(MSD)}}{\mathrm{d}t}. \tag{6}$$

In other words, the time derivative of the MSD gives the diffusion constant of the relevant species. Then the first-principles MD can in this way compute the H diffusion coefficient at different temperatures.

Molecular dynamics is classified with different constraints. Because we are dealing with many statistical averages, the constraints often correspond to different statistical ensembles. For example, one often adopted constraint set is the NVT, meaning particle number (N), volume (V), and temperature (T) are held constant in the simulation. This corresponds to the well-known canonical ensemble often encountered in statistical physics.

An apparent feature of molecular dynamics computation is its statistical nature. This is due to the fact that a many-body system is being treated and therefore the result could be quite different due to a slight change of parameters and assumptions. Take the hopping the H in the metal lattice as an example. The hopping from one octahedral site to the next is a small-probability event. In real life it may take many, say 10^{10}, attempted bumps before a real jump can happen. Therefore, a variety of assumptions must be made to expedite the real simulation. Such assumptions cause a spread in the calculated results, sometimes could be fairly broad. Fortunately for many circumstances of MD, the mean objective is to obtain an order-of-magnitude estimate or a qualitative understanding. Hence, as long as the simulation can help us understand and predict, the MD study is then considered valuable. Figure 9 demonstrates some simulation results of H diffusion in Pd. The match with the experiment is better at higher temperature. At lower temperature, the MD results tend to underestimate the rate due to the fact that quantum tunneling brings additional hopping terms into the diffusion constant.

6. Dislocations Defects and their Effects

Linear defects or dislocations in a metal are known to generate a range of interesting phenomena. One possible consequence of have such a dislocation on H or D is to act as a potential trap so that the local effective density of very high localized H/D densities (terms "deuterium clusters"). However, so far there has not existed direct experimental evidence for such a trap of high H/D density, also very convincing circumstantial evidence reported in [4,5]. Theoretical studies of the condensation process for cluster formation have also been presented [22]. Because this is a small-scale phenomenon on the Angstrom level, existing spectroscopic and microscopic means are not powerful enough to observe it directly, deep inside the metal and often under high internal pressure.

Because of the limitation of the current experimental techniques, the first-principles MD is expected to play a critical role in understanding the effect of dislocations on hydrogen transport in metals. For example most of the metal hydrides utilized in modern batteries and fuel cells are high in the crystal defects. In essence, a perfect crystal of metal hydride

is for most time a rather poor hydrogen storage for rechargeable battery or fuel cell electrodes. This is because the hydrogen is then tightly bonded to the metal lattice, causing very slow diffusion. Meanwhile the high-power-density demand of modern electrochemical devices requires very fast ionics, which can only be furnished with a large amount of crystal defects in the hydride.

Due to the local trapping property of dislocations, it is natural to think about a high density accumulation of H/D, or cluster. We have attempted some preliminary MD simulation of such a situation. So far, the results have not been able to reproduce the conjectured structure that could be inferred from a variety of experiments. This work on density accumulation is continuing and will be reported later.

The first-principle simulations of defects are typically time-consuming. Because defects typically lack adequate periodicity at small scales, the simulation often involves large number of atoms and therefore is computational intensive. Nevertheless by proper choice of the structure one can simulate many properties with modest computational tools. Figure 10 is one example of dislocation along the FCC [2 1 1] direction. The hydrogen diffusion in Pd is well known to be affected by the presence of dislocations [23–25]. However, the exact mechanism with which the mobility of H is affected still remains unclear and therefore consists of an interesting topic. It is intuitive to conjecture that the diffusion constant is significantly different normal and parallel to the dislocation direction. The authors have started some preliminary investigations of the defect properties and effects with MD simulations. The initial results are qualitatively matched to the experiments cited in [4]. The details will be published elsewhere.

7. Conclusions

Detailed FLAPW electronic structure calculations carried out for H at various sites and compositions of PdH_x provides the following insights of importance to the metal hydride and LENT communities. It is confirmed that H hopping through tetrahedral sites is energetically more favorable than through bridging sites. H drifting appears to involve a partially charged positive ion because the proton attracts extra negative charge in its hopping path, which partially screens out the unit positive charge carried by the proton. Charge accumulation around the bridging site is shown to be relatively large and thus must be considered in evaluating catalytic properties associated with PdH surfaces and reactive sites. Preliminary studies of dislocation defect trap sites for hydrogen and deuterium are also presented.

References

[1] D.P. Smith, *Hydrogen in Metals*, The University of Chicago Press, Chicago, 1948.
[2] F.A. Lewis, *The Palladium–Hydrogen System*, Academic Press, New York, 1967.
[3] N.F. Mott and H. Jones, *Theory of the Properties of Metals and Alloys*, Dover, New York, 1958.
[4] G. H. Miley and X. Yang, *Fusion Sci. Technol.* **56** (1), 395–400
[5] L. Holmlid, H. Hora, G. Miley and X. Yang, *Laser and Particle Beams* **27**(3).
[6] P. Hohenberg and W. Kohn, *Phy. Rev*. **136** (1964) B864.
[7] P. Tripodi, M.C.H. McKubre, F.L. Tanzella, P.A. Honnor, D. Di Gioacchino, F. Celani and V. Violante, *Phys. Lett.* A **276** (2000) 122.
[8] G.H. Miley, G. Selvaggi, A. Tate, M. Okuniewski, M. Williams, D. Chicea, H. Hora and J. Kelly, in *Proc.ICCF-8*, Villa Marigola, Lerici (La Spezia), Italy, 2000, p. 169.
[9] C. Wagner and G. Heller, *Z. Phys. Chem.* B **46** (1940) 242.
[10] H. Wipf, *Hydrogen in Metals* (Part II), in G. Alefeld and J. Volkl (Eds.), Springer–Verlag, Berlin, 1978, p. 273.
[11] R. Pietrzak, R. Szatanik and M. Szuszkiewicz, *J. Alloys Comp.* **282** (1999) 130.
[12] A.C. Switendick and Ber. Bunsenges, *Phys. Chem.* **76** (1972) 535.
[13] D.A. Papaconstantopoulos, B.M. Klein, J.S. Faulkner and L.L. Boyer, *Phys. Rev.* B **18** (1978) 2784.
[14] M. Gupta and A.J. Freeman, *Phys. Rev.* B **17** (1978) 3029.
[15] C.T. Chan and S.G. Louie, *Phys. Rev.* B **27** (1983) 3325.

[16] C. Elsasser, M. Fahnle, K.M. Ho and C.T. *Chan, Phys*. B **172** (1991) 217.
[17] C. Elsasser, K.M. Ho, C.T. Chan and M. Fahnle, *J. Phys. Condens. Matter* **4** (1992) 5207.
[18] Y. Wan, S.N. Sun and M.Y. Chou, *Phys. Rev*. B **53** (1996) 1.
[19] N. Luo, G. H. Miley and A. G. Lipson, *Appl. Surface Sci.* **219** (2003)167.
[20] WIEN2K, http://www.wien2k.at.
[21] C. Elsasser, K.M. Ho, C.T. Chan and M. Fahnle, *Phys. Rev.* B **44** (1991) 10377.
[22] Yeong E. Kim, *Naturwissenschaften* **96** (2009) 803–811.
[23] S.B. Gesari, M. E. Pronsato and A. Juan, *Int. J.Hydrogen Energy* **34** (2009) 3511.
[24] B.J. Heuser and J.S. King, *Metall. Mater. Trans. A-Phys. Metall. Mater. Sci*. **29** (1998) 1593.
[25] B.J. Heuser, T.J. Udovic and H. Ju, *Phy. Rev*. B **78** (2008) 214101.